KEY STRUCTURES OPTIMIZATION OF SPHERICAL BLOWOUT PREVENTER BASED ON MULTIPLE REGRESSION ANALYSIS

Yinfang Fan[1], Yan Chen[1,*], Fangxu Yao[2], Hong Zhuo[3]
[1]School of Information and Mathematics, Yangtze University, Jing Zhou, 434023, China;
[2]SJ petroleum machinery CO. SINOPEC Oilfield Equipment Corporation,Jing Zhou, 434000, China;
[3]Changqing Division, China National Logging Corporation,Xian, 710201, China.
Email: 520050@yangtzeu.edu.cn

Abstract As the important equipment in the field of well control, the spherical blowout preventer can quickly close the wellhead when a blowout accident occurs. In this paper, the spherical blowout preventer of FH28-35 is taken as the research objects, and the maximum stroke and maximum extrusion volume of the spherical blowout preventer are calculated by geometric methods. Based on the theoretical analysis and experimental data, the mechanical behaviour of the spherical blowout preventer during well sealing was analysed, the equivalent stress and contact pressure distribution law of the rubber core were summarized. The finite element model of the spherical blowout preventer was established based on the polynomial regression analysis, the simulation results were input into the Design-Expert software, and the residual analysis was carried out. Finally, the optimal combination of the three response factors was analysed. The results show that the equivalent stress of the core of the spherical blowout preventer is reduced when the core is optimized without affecting the sealing effect, which can effectively prolong the life of the core.

Keywords: Blowout preventer; Structures optimization; Equivalent stress; Sealing effect; Residual analysis; Multiple regression.

1.Introduction

Spherical blowout preventer (Referred to as BOP) is a set of well-control equipment of widely used on oil and gas fields, spherical rubber core is the main components. But in recent years, spherical rubber core has low service life and bad sealing performance due to various reasons, can't meet the demand of drilling operation. The spherical rubber core's mechanical behaviour, namely the deformation and failure regularity of the rubber core in the process of sealing the well was studied. Yao et al. [1-3] simultaneously used computer simulation and theoretical calculation methods to compare and analyze the mechanical behaviour of rubber core sealing of annular blowout preventer. The two methods have the same change rule of rubber core contact pressure, which proves the feasibility of computer simulation and theoretical calculation method. Lin et al. [4-6] established the finite element model of the annular blowout preventer after wear and simulated and analyzed the eccentric wear of the inner cavity of the annular blowout preventer. The results show that eccentric wear defects will lead to new stress concentration points in the annular blowout preventer, and its depth is positively correlated with the structural safety of the annular blowout preventer. Yang et al. [7,8] established a three-dimensional model of the rubber core, calculated the finite element of the rubber core through ABAQUS software, obtained the stress distribution law of the rubber core during tripping, and proposed and verified the optimization scheme. Guo et al. [9-12] established a three-dimensional finite element model of the rubber core was by ABAQUS software to simulate the dynamic sealing process. Wu et al. [13,14] established the model of FZ35-105 blowout preventer and carried out finite element calculation. Using the response surface method and taking the equal effect force as the response value, the interaction law of the length, width and height of the blowout preventer shell on the mechanical properties of the blowout preventer was obtained. Through the quadratic response surface model, the structure of the gate plate blowout preventer was optimized [15].

https://doi.org/10.17683/ijomam/issue19

In order to solve the above problems, a real spherical BOP model is established in this paper. The basic mechanical experimental data of nitrile butadiene rubber are fitted by ABAQUS software, and the Yeoh constitutive model that can express the large deformation of rubber is optimized. Based on the multiple regression analysis, the response surface method was used to optimize the structure of rubber core and supporting rib. The optimization results further revealed the general law of stress-strain of annular rubber core, provided a reference for the structural optimization design of annular rubber core, and greatly helped to improve the service life of rubber core.

2. Structure and Work Principle of Spherical

The structure diagram and work principle diagram of spherical blowout preventer is shown in Fig.1. The spherical blowout preventer is mainly composed of a head cover, housing, a piston, and rubber core and support rib. During the working process of the spherical blowout preventer, the piston moves upward to push the rubber core to extrude and deform, and seal the drill pipe to achieve the purpose of sealing the well.

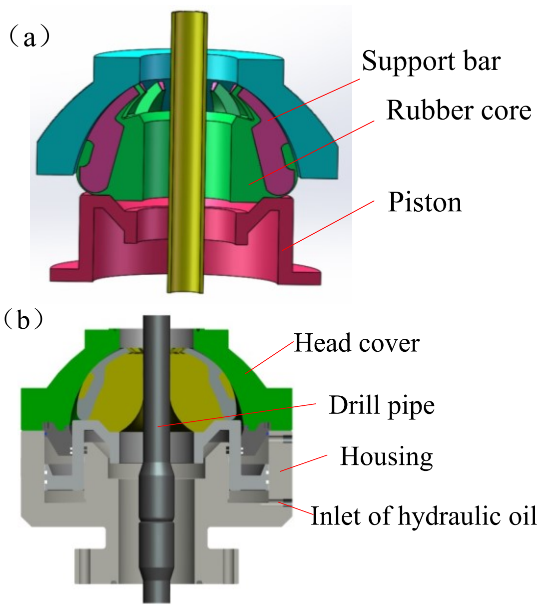

Figure 1: Structure and work principle diagram of spherical blowout preventer.

Fig. 2 is the failure photos of the rubber core and support rib. The rubber core between the support rib and the piston of the spherical blowout preventer is relatively thin, and the bottom of the rubber core bears an instantaneous load during work, and the rubber core is easy to crushing and tearing, as shown in Fig. 2（a）. The structural design of the support rib is unreasonable, and it will fracture under the extrusion and bend forces, as shown in Fig. 2（b）.

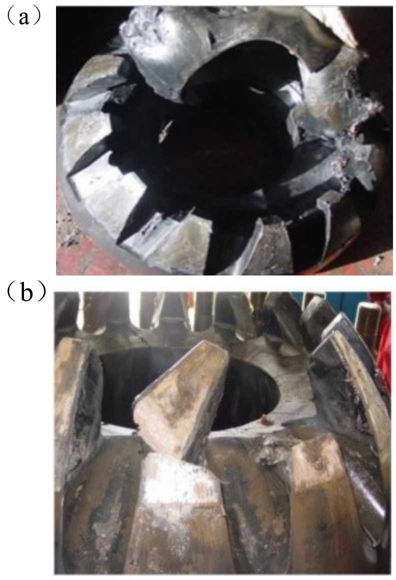

Figure 2: Failure photos of rubber core and support rib: (a) rubber core, and (b) support rib.

The sealing parameters of the spherical BOP are calculated in the same way as the spherical BOP, and the core idea is that the volume of the rubber core remains unchanged before and after deformation.

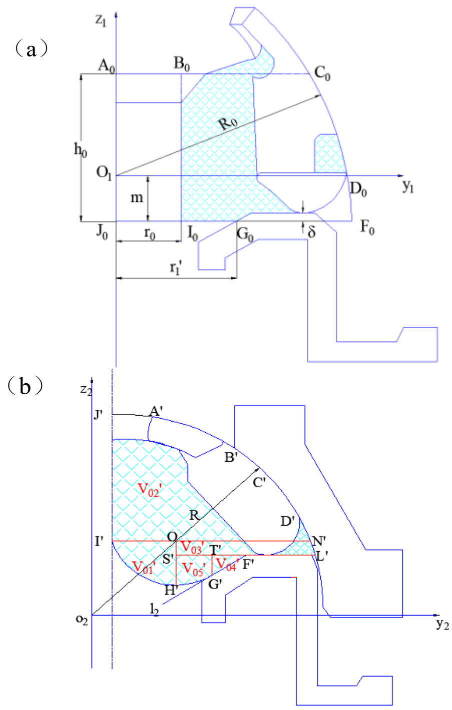

Figure 3: Profile diagrams of the spherical blowout preventer before and after deformation: (a)before and (b)after.

As shown in Fig. 3, V_0 is equal to the volume of the rotating body generated by the rotation of the plane figure enclosed by the $B_0C_0D_0F_0I_0$ around the z_1 axis, which is approximately the difference between the volume of one cylinder table and the volume of two cylinders. V_{01}, ... V_{04} is a plane figure surrounded by arc C_0D_0 and straight lines $z_1=Z_{A0}$, $Z_1=0$ and z_1 axis, polygonal $O_1D_0F_0J_0$, rectangular $A_0B_0I_0J_0$, and the volume of the rotating body formed by the rotation of polygon $D_0F_0G_0$ around the z_1 axis.V_{01}', ... V_{05}' is the volume of the rotating body formed by the rotation of the polygon

OH′I′O, the polygonal J′A′N′I′, the polygonal ON′L′S′, the polygonal T′F′G′, and the polygonal S′T′G′H′ by rotating the z_2 axis once in one rotation. The volume of the core V_0' is equal to the volume of the rotating body generated by the rotation of the plane figure enclosed by J′A′N′L′F′G′H′I′ ar$_o$und the z_2 axis.Because the plane figure enclosed by arc $B'L'$、$B'B'''$ and $B'''L'$ rotates around the z_2 axis, the volume of the rotating body generated is:

$$V'_{06} = \pi\int_{Z_{F'}}^{Z_{B'}} y_2^2 dz_2 - \pi r_0^2 (z_{B'} - z_{F'}) \tag{1}$$

So the amount of extrusion:

$$V'_{Extruded} = V_0 - V'_{06} = V_0 - \pi\int_{Z_{F'}}^{Z_{B'}} y_2^2 dz_2 + \pi r_0^2 (z_{B'} - z_{F'}) \tag{2}$$

And because:

$$z_{B'} = \sqrt{R^2 - r_0^2}, y_2^2 = R^2 - z_2^2 \text{ (On the arc B′L′)}$$

Therefore, the piston stroke allowed by the spherical core in the work is H′max, and the extrusion amount of the spherical core is called the maximum extrusion amount. The maximum dispensing volume:

$$V'_{Extruded} = V_0 - \pi(R^2 - r_0^2)$$
$$(\sqrt{R^2 - r_0^2} - z_{F'}) + \frac{\pi}{3}[(\sqrt{R^2 - r_0^2})^3 - z_{F'}^3]$$

Therefore, the maximum extrusion amount of the core of FH28–35 spherical BOP is 24399386.86mm^3, which is about 24.40L.

3. Constitutive Model of the Core Material of the Spherical BOP

The mechanical behavior of rubber is usually studied in experiments by uniaxial tension and uniaxial compression [16]. According to the relevant regulations a total of 6 dumbbell–shaped samples were prepared of nitrile rubber [17,18], with a length of 65±0.5 mm and a height of 10±0.5 mm, and a total of 6 rectangular samples of nitrile rubber were prepared, with a length of 55±0.5 mm and a height of 7.5±0.5 mm as shown in Fig. 4. The uniaxial tensile test and the uniaxial compression experimental equipment are shown in Fig. 5.

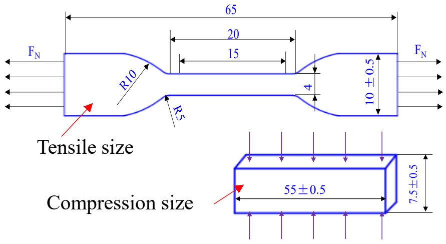

Figure 4: Specimen structural dimensions.

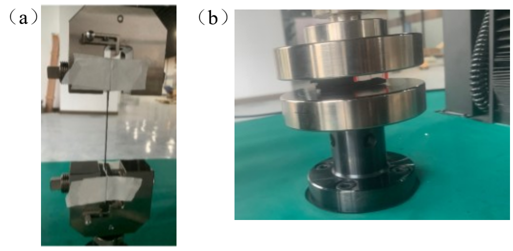

Figure 5: Specimen structural dimensions: (a)tensile test; (b)compression test.

The experimental data were fitted by ABAQUS software, and the constitutive model of rubber core material was optimized. According to Fig. 6, when the strain is small, all models are close to the experimental data, but when the nominal strain is 300%, it is found that Yeoh model is the most consistent with the experimental data. The rubber core of annular blowout preventer has large deformation during operation, so Yeoh model is selected as the constitutive model of rubber core material. According to the fitting results of ABAQUS software, the parameters of Yeoh constitutive model are: C_{10}=1.052 MPa，C_{20}=-0.325 MPa，C_{30}=0.227 MPa.

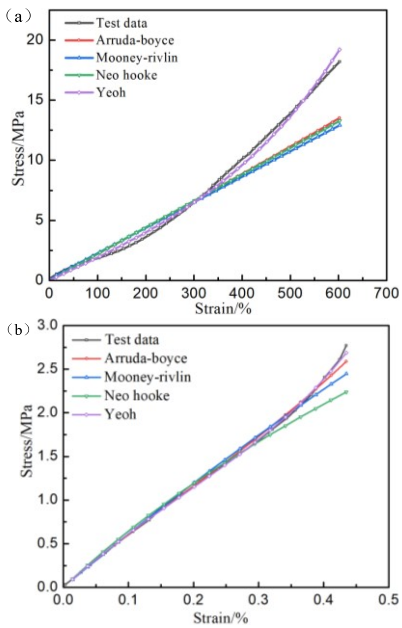

Figure 6: Experimental fitting results of core material: (a)tensile test, and (b) compression test.

4. Finite Element Calculation of Spherical BOP

The construction of the spherical BOP model is basically the same as that of the spherical BOP. Taking the FH28–35 spherical BOP as the research object, a 1/6 model of the spherical BOP was also established, as shown in Fig. 7(a). Endow support ribs, drill pipes, and rubber core materials with properties.

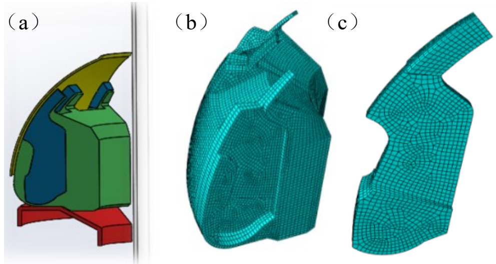

Figure 7: Finite element analysis model of blowout Preventer: (a)analysis model, (b) rubber core and (c) support ribs.

Material attributes: The drill pipe, support ribs, top cover and piston are all made of 35CrMo material, Yield strength of the material is 835 MPa, Young's modulus is 213GPa Poisson's ratio is 0.3. The rubber core is made of nitrile rubber, and the constitutive model is Polynomial second–order constitutive model, with a density of 1.5×10^{-9} tons/mm^3.

In order to simulate the process of sealing the drill pipe of the blowout preventer during the blowout, the boundary conditions are set: limit the displacement of the top cover and the drill pipe in the direction of U1 (X direction), U2 (Y direction) and U3 (Z direction), that is, the top cover and the drill pipe are completely fixed, and the displacement of the piston is 171.11mm, and the direction is the positive direction of U2. The top cap and piston are set to a rigid body. As shown in Fig. 7, the support rib and rubber core are special–shaped structures, and both use C3D8R meshes, which can effectively improve the calculation accuracy.

Fig. 8 shows the equivalent stress distribution of the core when the piston stroke is 4 mm, 42 mm and 171 mm, respectively. When the piston stroke reaches 4mm, the piston pushes the back of the rubber core, and the rubber elasticity makes only the bottom of the rubber core produce stress. The rubber core has been in contact with the top cover and moves in a circular motion along the spherical inner surface of the top cover when the piston stroke reaches 42mm, so the bottom of the rubber core and the back of the rubber core produce greater stress at the same time. The rubber core tightly holds the drill pipe when the piston stroke is 171mm, and the sealing area of the rubber core and the fillet adhesion with the plate on the supporting rib produce a large stress.

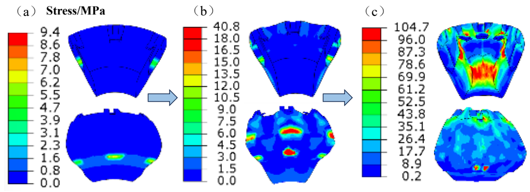

Figure 8: The equivalent stress of the core varies with the piston stroke: (a) 4mm, (b) 42mm and (c) 171mm.

Fig. 8 shows the stress distribution of the spherical rubber core when the piston reaches the maximum stroke. Under the joint extrusion of the top cover and the support ribs, the maximum stress is distributed in the middle end of the sealing area of the rubber core at mark 1, and the stress is 104.7MPa, which is within the range of the nitrile rubber. At marks 2 and 3, the spherical rubber core folds when it is in self–contact, and a gap occurs when the sealing area is in contact with the drill pipe, which will affect the sealing effect.

As shown in Fig. 9, the maximum equivalent stress of the support rib is concentrated at the bottom. And the bottom of the support rib is always subject to the power from the piston with the contraction of the rubber core to the center, the support rib rotates.

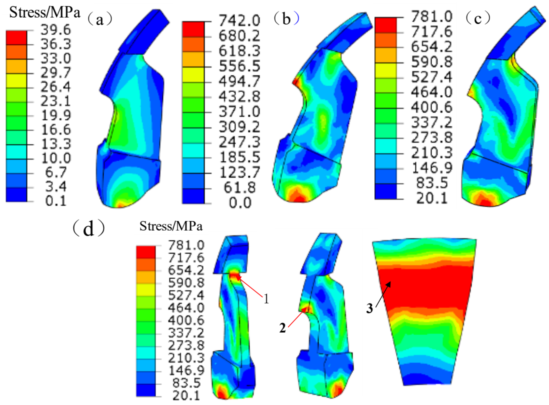

Figure 9: The support rib changes with the piston: (a)4mm, (b)42mm, (c)171mm, and (d) stress distribution.

As shown in Fig. 10, the stress distribution of the support rib when the piston reaches its maximum stroke. Marks 1, 2 and 3 are the fillets between the plate in the support rib and the rubber core. The life of the support ribs of the spherical BOP will be greatly reduced after repeated work under high temperature and high pressure. It is easy to break with the combined action of the top cover and piston.

The three paths are made along the outer surface of the drill pipe in Fig. 10. Path–1 is the axial direction of the drill pipe, Path–2 and Path–3 is the circumferential direction of the drill pipe. Fig. 11 shows the contact pressure distribution on the three paths, and the mid–end sealing effect of the sealing area is the best, and the maximum contact pressure between the drill pipe and the rubber core is 55.7MPa. The contact pressure at the upper end of the sealing area is small, about 45MPa, and the contact pressure in the middle of Path–2 has a significant trough, which is the area where the spherical rubber core is wrinkled by self–contact.

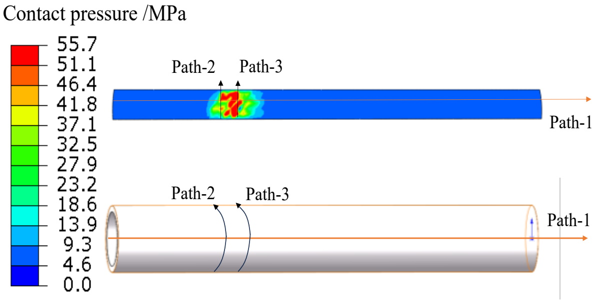

Figure 10: Contact pressure on drill pipe.

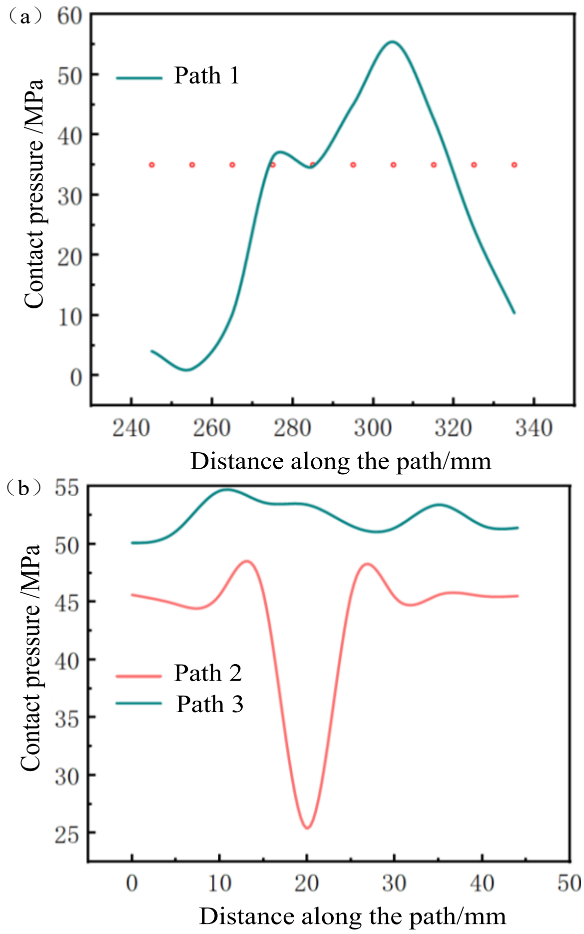

Figure 11: The contact pressure along the path on the drill pipe: (a)axial and (b) circumferential.

The curves in Fig. 12 are the equivalent stress and contact pressure curves of the middle end of the sealing area of the spherical BOP and the spherical BOP, respectively. Both blowout preventers can reach the rated contact pressure at the moment of load application, and both can effectively seal the wellhead and prevent blowout.

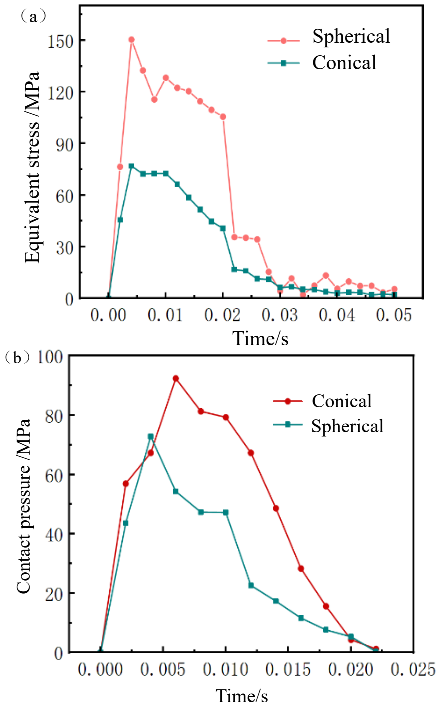

Figure 12: Stress and contact pressure distribution of the rubber core: (a) stress, and (b) contact pressure.

Because the rubber that wraps the bottom around the support ribs is too thin, the spherical BOP is easily squeezed and torn by the piston and the bottom of the support ribs under extreme impact loads. However, the supporting rib of the spherical blowout preventer is in contact with the rubber core and the bottom surface of the supporting rib is a large plane, so the rubber tear at the bottom of the rubber core of the spherical blowout preventer does not appear.

5. Optimization of the Structure of the BOP

The Design–Expert software was used to optimize the structure of the spherical BOP and the optimal design used a combination of three response factors and two response values [19,20]. The response factors are A, B and C. A is the width of the upper plate of the support rib, B is the radius of the upper plate, and Cis the sealing area of the rubber core, and the optimized structure has been marked in red. The response values are the maximum equivalent stress of the spherical core (hereinafter referred to as stress 3) and the maximum equivalent stress of the support rib (hereinafter referred to as stress 4).

According to the experiments designed by the software, the models of 17 groups of spherical BOP were established, and the finite element calculation was carried out by ABAQUS software.

The simulation results are input into the corresponding experimental group of Design–Expert software[21], and the response surface diagram and the ternary quadratic polynomial regression equation about the response factor can be obtained by Design–Expert software.

An R2 value close to 1 indicates that the model fits the data well. The R2 of stress 1of the pure quadratic function model, the cross-function model and the complete quadratic function model are 0.8346, 0.9122 and 0.9999, respectively, and the R2 corresponding to stress 4is 0.8398, 0.9698 and 0.9955, respectively. Therefore, a fully quadratic function model is selected as the regression model.

Fig. 13 shows the normal probability distribution of residuals, the distribution of residuals and predicted values, and the distribution of predicted values and actual values.

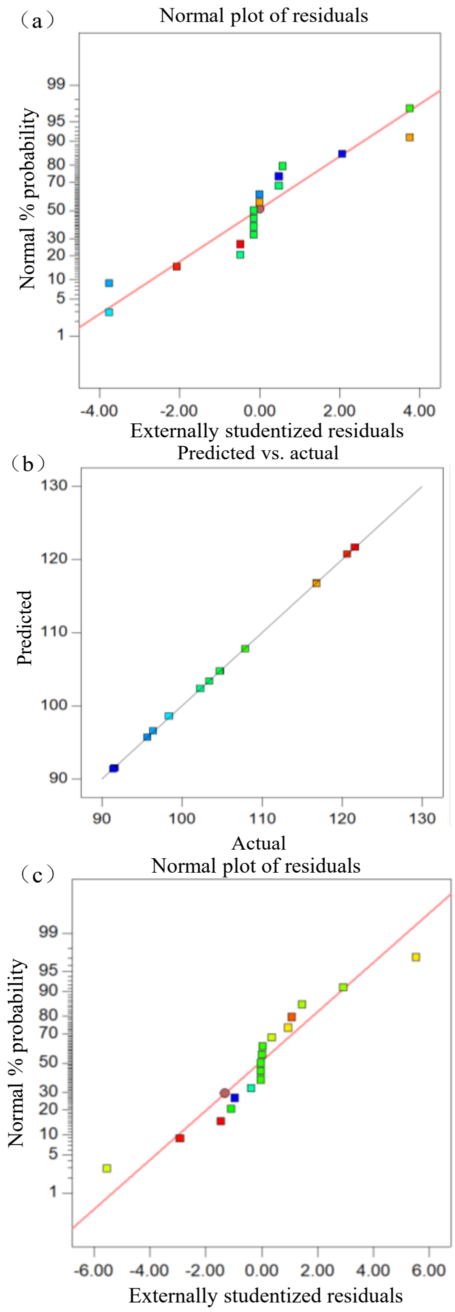

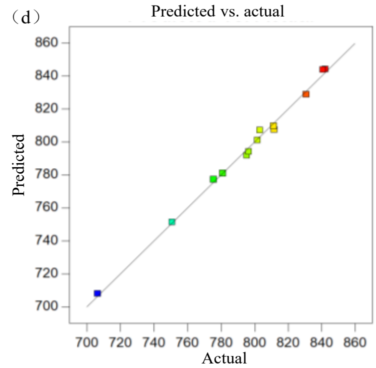

Figure 13: Residual analysis.

The regression equations for the fully quadratic model of stresses 3 and 4 solved by Design–Expert software are as follows:

$$F_3 = 104.72 - 2.04A - 2.55B - 12.59C$$
$$+0.15AB - 0.075AC - 0.050BC$$
$$-1.05A^2 - 0.67B^2 + 2.50C^2$$

$$F_4 = 781.06 - 25.55A + 0.51B + 25.31C$$
$$+0.65AB + 24.25AC + 13.43BC$$
$$+15.51A^2 + 22.08B^2 - 13.47C^2$$

Figs. 14 and 15 show the response surface and contour of stress 3 and stress 4 under the complete quadratic function model. The three response factors have an interactive effect on the response value.

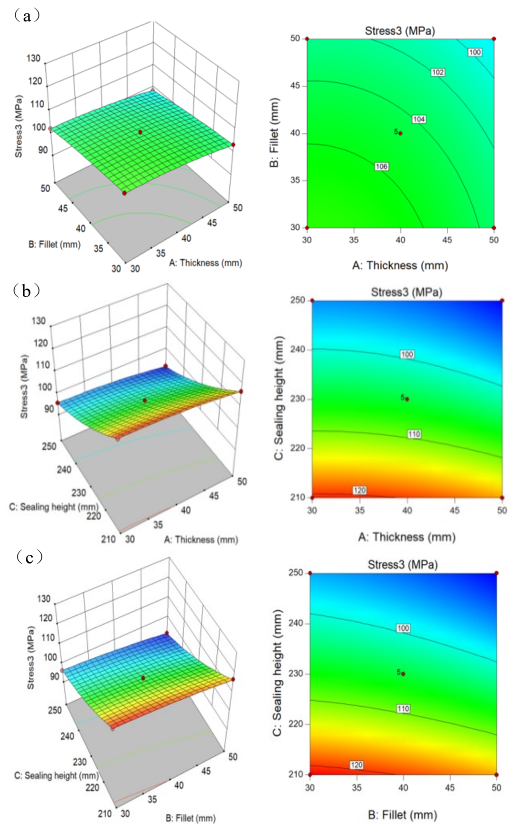

Figure 14: Stress 3 response surface and contour: (a)AB–stress 3, (b)AC–stress 3, and (c) BC–stress 3.

As shown in Fig. 14 (a), when the height of the sealing area is unchanged, stress 3 decreases with the increase of the radius of the fillet and decreases with the increase of the thickness of the upper plate. In Fig. 14(b), stress 3 decreases with the increase of the height of the sealing area when the radius of the fillet remains unchanged. Stress 3 decreases with the increase of the thickness of the upper plate, but the decrease is small. As shown in Fig. 14(c), when the thickness of the upper plate is unchanged, stress 3 decreases with the increase of the height of the sealing area. Stress 3 decreases with the increase of fillet radius, but the decrease is small. It indicates that the influence of the height of the sealing area is large, and the influence of the other two response factors is basically negligible.

As shown in Fig. 15(a), stress 4 decreases with the increase of the thickness of the upper plate when the sealing area remains unchanged, and, stress 4 decreases first and then increases with the increase of the corner radius when the thickness of the upper plate is 30 mm–40mm, but stress 4 is basically not affected by the radius of the fillet when the thickness of the upper plate is 40 mm–50mm. As shown in Fig. 15(b), stress 4 increases with the increase of the height of the sealing area when the radius of the fillet remains unchanged and has a greater influence when the height of the sealing area is 210mm–220mm, and stress 4 decreases with the increase of the thickness of the upper plate. As shown in Fig. 15(c), stress 4 increases with the increase of the height of the sealing area when the thickness of the upper plate remains unchanged, stress 4 decreases firstly and then increases with the increase of the radius of the fillet, and when the height of the sealing area is 230 mm–250mm, the stress 4 changes greatly with the increase of the radius of the fillet. It indicates that the thickness of the upper plate and the height of the sealing area have a great influence on stress 3 and stress 4, but they should be discussed in stages, and the influence on stress at different stages is different.

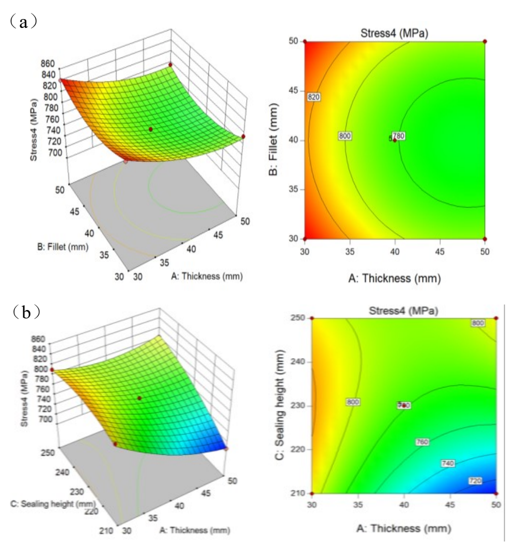

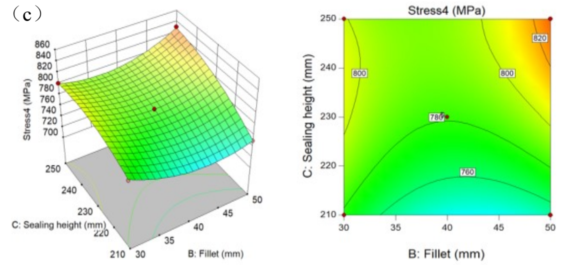

Figure 15: Stress 4 response surface and contour: (a)AB–stress4, (b)AC–stress 4, and (c) BC–stress 4.

According to the values of the three response factors of the optimal combination, the model of the spherical BOP was re–established, and the finite element calculation was carried out, and the stress distribution diagram of the rubber core and supporting ribs of the spherical BOP was obtained. As shown in Fig. 16, the equivalent stress optimization effect of the spherical BOP core is better, decreasing from 104.1MPa to 88.9MPa, a decrease of about 14.6%, which can effectively increase the life of the spherical core. The equivalent stress of the support ribs decreases from 781.0 MPa to 768.0 MPa.

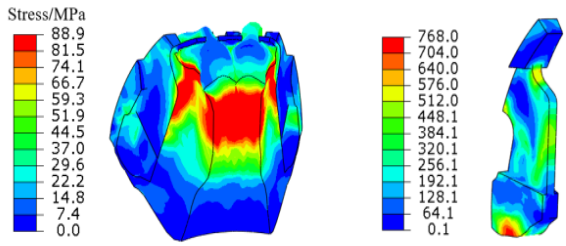

Figure 16: Stress contour of the rubber core and supporting ribs of the spherical BOP.

The pressure contour of the drill pipe and the circumferential and axial contact pressures along the path are shown in Figs. 17 and 18. After optimization, the contact pressure of the spherical core is reduced overall. The contact pressure at the top end of the spherical core is reduced to 45 MPa, and the middle end is reduced to 52.7 MPa, which is still higher than the rated working pressure. Therefore, the underground fluid can be sealed. So the improvement effect is relatively good.

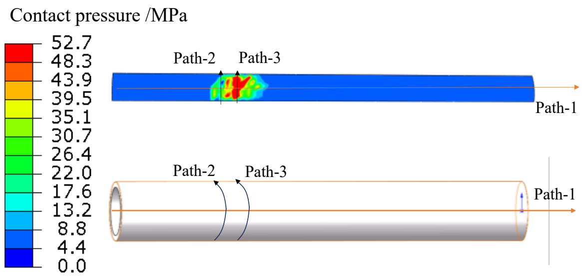

Figure 17: Contact pressure on drill pipe.

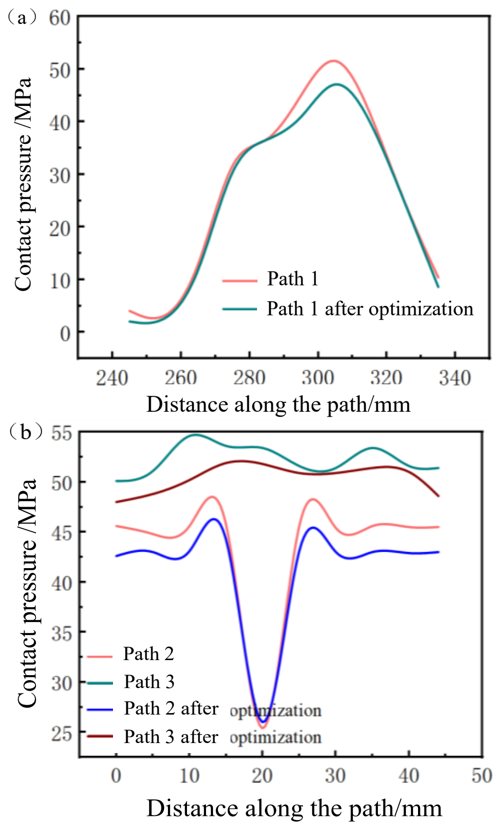

Figure 18: Contact pressure along the path on the drill pipe: (a) axial and (b) circumferential.

6. Conclusions

The spherical rubber core is in contact with the drill pipe when the piston displacement reaches about 60 mm. The contact pressure at the top end of the spherical core is slightly ahead of the middle end. The effective sealing length of the spherical core is about 60mm, which is shorter than that of the spherical core.

The equivalent stress and contact pressure curves of the middle end of the sealing area of the spherical BOP and the spherical BOP, respectively. Both blowout preventers can reach the rated contact pressure at the moment of load application, and both can effectively seal the wellhead and prevent blowout.

Because the rubber that wraps the bottom around the support ribs is too thin, the spherical BOP is easily squeezed and torn by the piston and the bottom of the support ribs under extreme impact loads. The influence of the height of the sealing area is large, and the influence of the other two response factors is basically negligible. The thickness of the upper plate and the height of the sealing area have a great influence on stress.

The height of the sealing area of the rubber core of the spherical BOP has a significant influence on the stress of the rubber core, and the height of the sealing area and the thicknesses of the upper plate have a significant effect on the support rib. After the optimization of the response surface method, the equivalent stress of the spherical BOP core decreased by 11.4%, and that of the spherical BOP core decreased by 14.6%.

References

[1] Yao Yao, Mao Zhengyi, QI Yaoguang, et al. Analysis of Large Deformation of Sealing Rubber Core of Air-controlled Annular Blowout Preventer[J]. Lubrication Engineering50 (2019) 44(2): 39-44. https://doi.org/10.3969/j.issn.0254-0150.2019.02.007

[2] Li Wang, Tang Yang, He Yufa. Simulation and experimental analysis of critical stress regions of deep-water annular blowout preventer[J]. Engineering Failure Analysis106 (2019) 104161.https://doi.org/10.1016/j.engfailanal.2019.104161

[3] Lin Tiejun, Mou Yisheng, Lian Zhanghua, et al. Finite element analysis of fracture of a ram BOP for deep gas wells[J]. Engineering Failure Analysis98 (2019) 109-117.https://doi.org/10.1016/j.engfailanal.2019.01.083

[4] Lin Zhenhao, Yu Longjie, Hua Tingfeng, et al. Seal contact performance analysis of soft seals on high-pressure hydrogen charge valves[J]. Journal of Zhejiang University-SCIENCE A23 (2022) 247–256. https://doi.org/10.1631/jzus.A2100395

[5] Liu Yang, Qian Liqin, Xia Chengyu, et al. Design and experimental study on a novel sealing structure of rotary control head for coalbed methane underbalanced drilling[J]. Engineering Failure Analysis139 (2022) 106441. https://doi.org/10.1016/j.engfailanal.2022.106441

[6] Dong Liangliang, Tang Yuan, Tang Geng, et al. Sealing performance analysis of rubber core of annular BOP: FEM simulation and optimization to prevent the SBZ[J].Petroleum9 (2023) 419-426. https://doi.org/10.1016/j.petlm.2021.12.001

[7] Yang Hai, Dong Liangliang, Yu XiangJun, et al. Study on sensitivity of annular BOP parameters to sealing performance in gas well snubbing service[J]. Mechanical Engineering Journal8 (2021) 20-00533. https://doi.org/10.1299/mej.20-00533

[8] Wang Jinlong, Ma Dudu, Xia Yun, et al. Failure mechanism analysis of ram BOP in HTHP gas well and mitigation measures[J]. Engineering Failure Analysis140 (2022) 106554. https://doi.org/10.1016/j.engfailanal.2022.106554

[9] Guo Lianglin, Zeng Yijin, Huang Jian, et al. Fatigue optimization of rotary control head rubber core based on steady sealing[J]. Engineering Failure Analysis132 (2022) 105935. https://doi.org/10.1016/j.engfailanal.2021.105935

[10] Wang Yue, Zou Longqing, Zhang Zongxu, et al.Research on Constitutive Model of Sealant Core for Annular BOP[J]. Machine Tool & Hydraulic50

(2022) 46-49. https://doi.org/10.3969/j.issn.1001-3881.2022.14.008

[11] Liu Weimin. Analysis and Optimization of Rubber Core Structure of Rotary BOP[J]. PETROLEUM MACHINERY49 (2021) 0(2): 7-14. https://doi.org/10.16082/j.cnki.issn.1001-4578. 2021. 02. 002

[12] Javed Akbar Khan, Sonny Irawan, Ahgheelan Seela Thurai, et al. Quantitative analysis of blowout preventer flat time for well control operation: Value added data aimed at performance enhancement[J]. Engineering Failure Analysis120 (2021) 104982. https://doi.org/10.1016/j.engfailanal.2020.104982

[13] Wu Ningpan, Zhang Jie, Zhang Chuan, et al. Optimal design of blowout preventer shell based on response surface methodology[J]. Technology Supervision in Petroleum Industry39 (2023) 48-52+77. https://doi.org/10.20029/j.issn.1004-1346.2023.03.010

[14] Zhang Jie, Li Qinchao, Zhang Chuan, et al. Sealing performance and failure mechanism of rubber core for conical blowout preventer during the well shut-in process[J]. Strength, Fracture and Complexity16 (2023) 1-19. https://doi.org/10.3233/SFC-230007

[15] Hu Gang, Wang Mingcheng, Wang Guorong, et al. Sealing performance and failure mechanism analysis of packing unit used in rotary blowout preventer for under-balanced drilling[J]. Engineering Failure Analysis129 (2021) 105654. https://doi.org/10.1016/j.engfailanal.2021.105654

[16] Liu Yang, Qian Liqin,Xia Chengyu,et al. Failure analysis and structural optimization of rubber core and support rib of full-size spherical blowout preventer[J]. Engineering Failure Analysis143 (2023) 106865. https://doi.org/10.1016/j.engfailanal.2022.106865

[17] Liu Yang, Lian Zhanghua. Failure analysis on rubber sealing structure of mandrel hanger and improvement in extreme environments[J]. Engineering Failure Analysis125 (2021) 105433. https://doi.org/10.1016/j.engfailanal.2021.105433

[18] Liu Yang, Qian Liqin, Zou Jiayan, et al. Study on failure mechanism and sealing performance optimization of compression packer[J]. Engineering Failure Analysis136 (2022) 106176. https://doi.org/10.1016/j.engfailanal.2022.106176

[19] Zhang Jie, Li Qinchao, Zhang Chuan, et al. High-temperature sealing performance and structure optimization of rubber core for conical blowout preventer[J]. Engineering Failure Analysis234 (2024) 212606. https://doi.org/10.1016/j.geoen.2023.212606

[20] Li Junxiong, Xia Chengyu, Han Xueying, et al. Optimization of Performance of All-metal Hydraulic Oscillator by PB-BBD Response Surface Method[J]. Engineering Failure Analysis50 (2022) 35-39. https://doi.org/10.3969/j.issn.1001-3881.2022.18.008

[21] Qiao Tieliang, Guo Xin, Bai Yutian, et al. Optimization of Laser Cladding Process Parameters Based on Response Surface Methodology[J]. Techniques of Automation & Applications43 (2024) 22-26. https://doi.org/10.20033/j.1003-7241.(2024)07-0022-05